

# Influence of Off-Axis Loading of an Anterior Maxillary Implant: A 3-dimensional Finite Element Analysis

Ming-Lun Hsu, DDS, Dr Med Dent<sup>1</sup>/Fang-Ching Chen, DDS<sup>2</sup>/Hung-Chan Kao, PhD<sup>3</sup>/Cheng-Kung Cheng, PhD<sup>4</sup>

**Purpose:** To evaluate the influence of the stress/strain distribution in bone around an anterior maxillary implant using 2 types of bone and under 3 different loads. **Materials and Methods:** A premaxillary finite element model featuring an implant and its superstructure was created. Six different testing conditions incorporating 2 types of cancellous bone (high density and low density) under 3 different loading angles (0, 30, and 60 degrees) relative to the long axis of the implant were applied in order to investigate resultant stress/strain distribution. **Results:** The maximum equivalent stress/strain increased linearly with the increase of loading angle. For each 30-degree increase in loading angle, the maximum equivalent stress in cortical bone increased, on average, 3 to 4 times compared with that of the applied axial load. In addition to loading angle, bone quality also influenced resultant stress distribution. For the low-density bone model, a substantial strain in the cancellous bone was found not only near the implant neck but also at the implant apex. **Conclusion:** To achieve a favorable prognosis under off-axis loading of an anterior maxillary implant, careful case selection for appropriate bone quality and precise occlusal adjustment should be attempted to optimally direct occlusal force toward the long axis of the implant. INT J ORAL MAXILLOFAC IMPLANTS 2007;22:301-309

**Key words:** biomechanics, bone quality, dental implants, finite element analysis, off-axis load, premaxilla

With the predictability of dental implants for orofacial rehabilitation, the clinical use of oral and maxillofacial implants has rapidly expanded over the past 20 years.<sup>1-3</sup> In their retrospective study of 1,964 implants, Noack et al<sup>4</sup> reported that mandibular implants were generally more successful than maxillary implants. The overall preprosthetic loss rate was 1.9%, while 4.3% of implants were lost after prosthetic treatment.<sup>4</sup> In addition, osseointegration has

been achieved with early or immediate loading.<sup>5,6</sup> However, despite reports of relatively substantial success rates in many clinical studies, 100% success over the long term still appears unattainable.<sup>7</sup> Biomechanical factors play a substantial role in implant success or failure.<sup>8-10</sup> The application of occlusal forces induces stresses and strains within the implant-prosthesis complex and affects the bone remodeling process around implants.<sup>11,12</sup>

The amount of bone strain or stress is directly related to the amount of the occlusal force applied through the implant-supported prosthesis. From a cellular biomechanical standpoint, bone remodeling at the cellular level is controlled by the mechanical environment of strain.<sup>13</sup> Based on Frost's mechanostat concept, bone fractures at 10,000 to 20,000  $\mu$ strain (1% to 2% deformation). However, just 20% to 40% of the amount of strain required for fracture (ie, 4,000  $\mu$ strain) may trigger cytokine to begin a resorption response.<sup>14,15</sup> In other words, excessive bone strain may not only result in physical fracture but also cause bone resorption. The interaction of the mechanical and biologic factors in the oral environment is a critical determinant in the identification of

<sup>1</sup>Associate Professor and Associate Dean, Dental School, National Yang-Ming University, Taipei, Taiwan.

<sup>2</sup>Graduate Student, Dental School, National Yang-Ming University, Taipei, Taiwan.

<sup>3</sup>Assistant Research Scientist, Biomechanics Research Laboratory, Medical Research Department Mackay Memorial Hospital, Institute of Biomedical Engineering, National Yang-Ming University, Taipei, Taiwan.

<sup>4</sup>Professor, Institute of Biomedical Engineering, National Yang-Ming University, Taipei, Taiwan.

**Correspondence to:** Dr Ming-Lun Hsu, Associate Professor and Associate Dean, Dental School, National Yang-Ming University, No.155, Sec.2, Li-Non Street, Taipei, Taiwan. Fax: +886 2 28264053. E-mail: mlhsu@ym.edu.tw

**Table 1 Physical Properties of Different Components Used**

Component	Elastic modulus (GPa)	References
Cortical bone	13.0	Tada et al <sup>22</sup>
Cancellous bone		
High-density	1.37	Sevimay et al <sup>23</sup>
Low-density	0.8	Tepper et al <sup>18</sup>
Titanium (implant, abutment)	102	Tada et al <sup>22</sup>
Porcelain (crown)	67.2	Ishigaki et al <sup>24</sup>

unfavorable loading conditions that may result in an undesirable bone response and predictable bone loss.<sup>16</sup> To achieve optimized biomechanical conditions for implant-supported prostheses, conscientious consideration of the biomechanical factors that influence prosthesis success is essential.

Biomechanical factors play an important role in maintaining the bone-implant interface.<sup>10,17</sup> Although there are many critical mechanical factors related to implant failure, Tepper et al emphasized the importance of force direction.<sup>18</sup> In reality, occlusal force almost always features a transverse component in addition to a vertical component. Off-axis force, which is common during normal mastication, would appear to induce more stress than does axial force.<sup>19</sup> For the incisal region, the direction of the maximum incisal biting force is about 12 degrees toward the frontal plane, which means that the lateral component of force on an anterior dental implant can be appreciable.<sup>20</sup> Moreover, the placement of dental implants would be more likely to produce an unfavorable off-axis load in the case of severe palatal resorption of the alveolar ridge following tooth extraction than in the case of a ridge without resorption.

Although many studies have been conducted about the stress on implants, to the authors' knowledge, fewer such studies have related to stress analysis in the maxilla, and even fewer to the premaxillary region. In cases where esthetics requires tooth overlap in the anterior region, off-axis loading of the implant is usually unavoidable.<sup>21</sup> The bone quality in the premaxillary region is also typically not as good as that in the mandible. In addition, from a review of the literature it would appear that most finite element analyses have assumed that occlusal load was directly applied on the abutment of the dental implant. Such studies fail to consider the effect of a

prosthetic crown in a clinical setting. The application of load on a crown or implant results in the production of different bending moments; therefore, a more detailed premaxillary finite element analysis (FEA) model with an implant and its superstructure is necessary. The purpose of this study was to evaluate the influence of the stress/strain distribution in bone around an anterior maxillary implant using 2 types of bone and under 3 off-axis loads.

## MATERIALS AND METHODS

### Model Geometry

A model of a maxillary segment in the incisal region featuring an implant and its superstructure was constructed on a personal computer using a computer-aided design program (Pro/Engineer 2000i; Parametric Technology, Needham, MA). A dried human maxilla was used as a reference to model the geometry of the premaxillary region. The thickness of the cortical bone was assumed to average 1.0 mm, a figure that was established for the human maxilla used herein based on a computed tomographic image.

A simulated  $3.75 \times 13$ -mm cylindrical implant made of commercially pure titanium was used for this study. The implant was placed in the maxillary right central incisor area and apposed by cortical bone in the crestal region and by cancellous bone for the remainder of the implant-bone interface. The overall dimensions of the crown were 10 mm in height, 9 mm in mesiodistal length, and 6.7 mm in buccolingual width. The crown was attached to a 6-mm-high implant abutment featuring a 1-mm collar and a 5-mm profile.

### Material Properties

All materials used in this study were considered to be isotropic, homogenous, and linearly elastic. The physical properties of different components used in this study are illustrated in Table 1. Two types of bone quality were modeled by varying the elastic modulus for the cancellous bone in the software. Since the Young's modulus of the maxillary anterior region has been described as being between that of the posterior mandible and that of the posterior maxilla,<sup>25</sup> a Young's modulus of 1.37 GPa was used to represent high-density bone,<sup>23</sup> while a Young's modulus of 0.8 GPa was used to represent low-density bone.<sup>18</sup> Elastic moduli of 102.0 GPa and 13.0 GPa were used for the titanium implant<sup>22,26,27</sup> and the cortical bone,<sup>28</sup> respectively. Since porcelain is often the premier choice for implant superstructure for the incisal region, the superstructure for the present model was assumed to be a ceramic crown.<sup>24</sup>

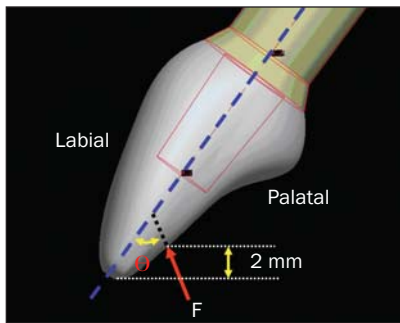


**Fig 1** The direction and location of the loading force. F = force;  $\theta$  was either 30 or 60 degrees.

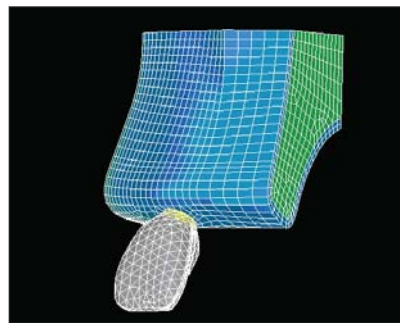


**Fig 2a** Oblique view of the FEA model.

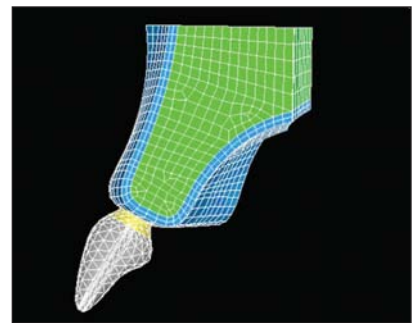


**Fig 2b** Sagittal view of the FEA model.

### Interface Conditions

The bone-implant interface was assumed to be perfect, simulating complete osseointegration, and the dental implant, abutment, and crown were assumed to be connected as a single unit.

### Constraints and Loads

The implant model was constrained in all directions at the nodes on the distal end and upper surface of the bone segment.

To evaluate the influence of force direction, the implant was assumed to be subjected to 3 different loading angles independently (0, 30, and 60 degrees relative to the long axis of the implant; Fig 1). To ensure that the axial force was directed along the long axis of the implant, a load of 178 N was directly applied on the occlusal node of the implant at the center of the abutment.<sup>29</sup> For off-axis loading, an occlusal load of 178 N was applied on a node at the crown. A 2-mm overbite was simulated to mimic clinical conditions. Thus, a model featuring 6 conditions was created by varying the elastic modulus in cancellous bone and introducing 3 different angled forces.

### Elements and Nodes

When the geometry of the model was complete, a specialized mesh-generation procedure was used to discretize the model (Figs 2a and 2b). To ensure the validity of the stress analysis, convergence testing of FEA model was conducted by applying element refinement methodology. This approach resulted in a model composed of 16,704 elements and 21,675 nodes.

### Stress/Strain Analyses

The Ansys software program (ANSYS 5.0; ANSYS, Canonsburg, PA) was used to calculate the von Mises equivalent (EQV) stress/strain in cortical and cancellous bone as well as in the implant. EQV stress/strain distributions for the models were illustrated by

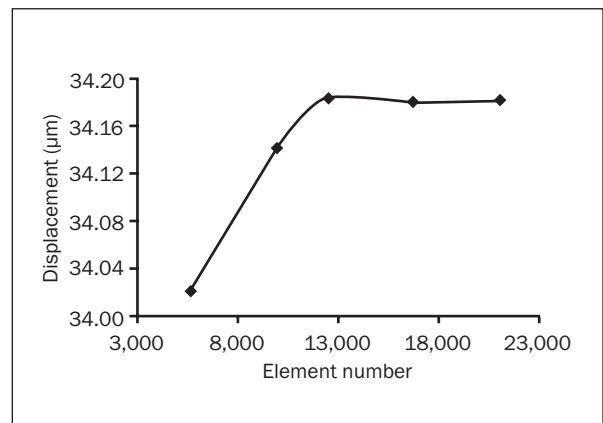


**Fig 3** The results of convergence testing for modeled high-density bone under off-axis loading (30 degrees) of 178 N. With the number of the elements increasing, displacement of the dental implant tended to level off.

means of contour mapping. The principal stress distribution around the implant-bone interface was displayed along the labial-palatal section.

## RESULTS

### Convergence Tests

The results of convergence testing for the high-density bone under off-axis loading (30 degrees) are presented in Fig 3. The total displacement of the dental implant, measured at the implant-abutment junction, was 34.2  $\mu\text{m}$  for the high-density model under a 30-degree off-axis loading of 178 N.

### Maximum EQV Stress/Strain Distribution in Bone

EQV stress/strain patterns were displayed as a contour line, with different colors connecting points of EQV stress level between certain ranges.

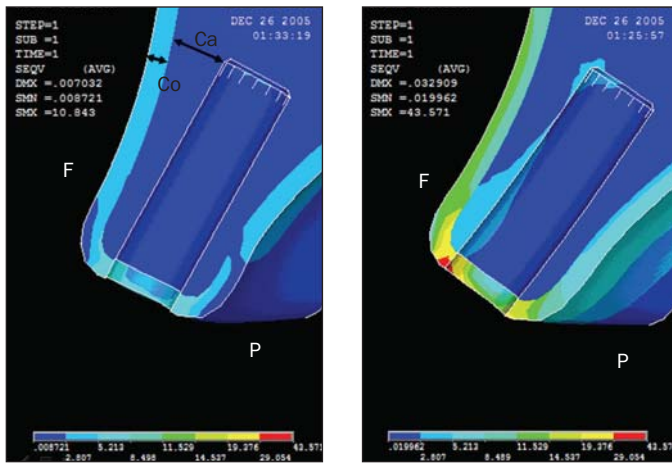


**Fig 4** EQV stress distribution in high-density bone under (left) 0-degree axial loading and (right) 30-degree off-axis loading. Sagittal view. F = facial side, P = palatal side, Co = cortical bone, Ca = cancellous bone.

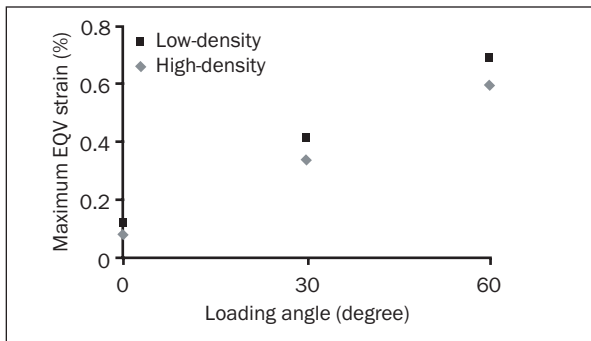


**Fig 5a** Maximum EQV strain for cortical bone. For axial loading (0 degrees), the percentage of change compared to the bone strain without loading is shown.

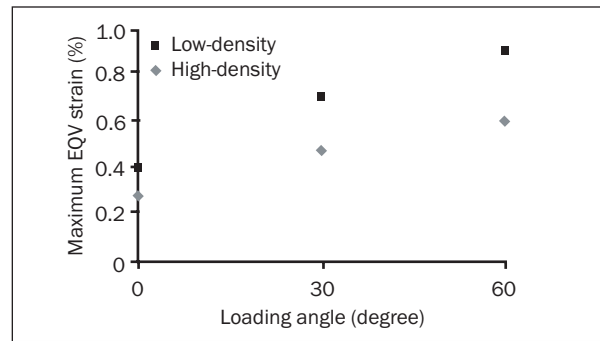


**Fig 5b** Maximum EQV strain for cancellous bone. For axial loading (0 degrees), the percentage of change compared to the bone strain without loading is shown.

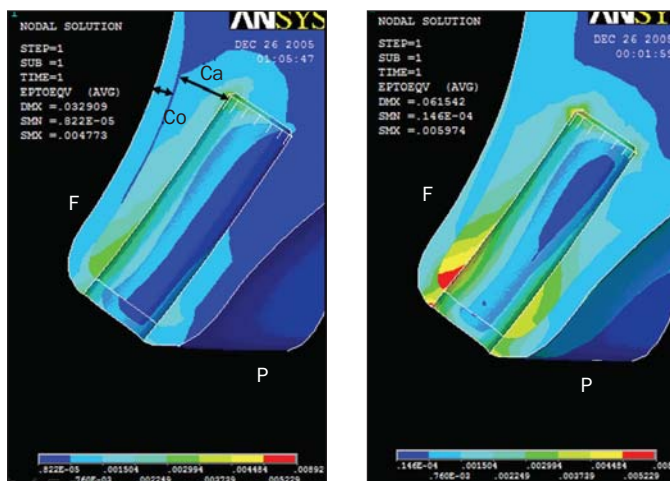
**Cortical Bone.** Compared with cancellous bone, substantial stress was observed in cortical bone. For all loading conditions, apart from axial loading, the maximum level of EQV stress was concentrated in the cortical bone and was observed on the labial side of the implant neck (Fig 4). For the high-density bone model, the maximum EQV stresses were 11 MPa, 44 MPa, and 76 MPa at angles of 0, 30, and 60 degrees, respectively. For the low-density bone model, the maximum EQV stresses were 16 MPa, 53 MPa, and 88 MPa at these angles. The stress developed under off-axis loading conditions was significantly greater than that produced under axial loading. For each 30-degree increase in loading angle (from 0 degrees), the maximum EQV stress developed in cortical bone increased, on average, 3 to 4 times compared with the axial load. The maximum EQV strain in cortical bone was plotted in Fig 5a. Regardless of load direction, the maximum EQV strain for low-density bone was always greater than the corresponding figure for high-density bone.

**Cancellous Bone.** The maximum EQV strain in the cancellous bone was plotted in Fig 5b. Under the same loading angle, the maximum strain in the low-density bone was higher than that in the high-density

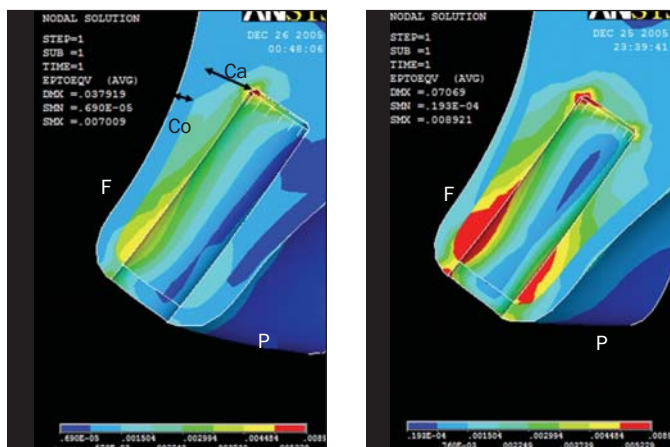
bone. As in the cortical bone, the strain increased as the loading angle increased, regardless of the bone quality. However, the patterns for EQV strain distribution in the cancellous bone showed some differences under loading, depending upon differences in force angle and bone quality. Compared with the high-density bone model, strain was distributed over a larger area around the implant apex in the low-density bone (Figs 6a to 6d). For example, under 60% off-axis loading, a rather substantial strain was seen to develop not only around the implant neck but also near the implant apex in the low-density bone (Figs 6c and 6d). Under each of the 6 test conditions, the maximum EQV strain in the cancellous bone was observed near the implant apex.

**Implant and Porcelain Crown.** Under axial loading conditions, the stress in the implant itself was concentrated at the loading point, although under off-axis loading, the stress that developed within the implant was concentrated at the implant-abutment interface. For models with the same bone quality, the EQV stress that developed at the implant-abutment interface under 30-degree off-axis loading proved to be about 200% of that developed under 60-degree off-axis load-

**Figs 6a and 6b** EQV strain distribution in high-density bone under (left) 30-degree off-axis loading and (right) 60-degree off-axis loading. Sagittal view.



**Figs 6c and 6d** EQV strain distribution in low-density bone under (left) 30-degree off-axis loading and (right) 60-degree off-axis loading. Sagittal view. The same color bar is used in these 4 figures except for the value given for dark blue in each figure (and the next-darkest blue in 6c). The maximum von Mises EQV strain of 8924  $\mu$ strain was noted near the implant apex in the low-density model.



ing. The stresses developed in the crown under off-axis loading were concentrated not only at the occlusal contact point but also at the crown-abutment interface.

### Principal Stress Distribution in Bone

The maximum tensile and compressive stresses that developed in bone around the dental implant are listed in Table 2. Positive values represent tensile stresses; negative values represent compressive stresses. To comprehend the stress distribution at the implant-bone interface, the maximum and minimum principal stress level distributions at the implant-bone interface along a labial-palatal section (Fig 7) were compared under axial loading and 60% off-axis loading (Figs 8a and 8b). The stress distribution at the implant-bone interface appeared to vary less and to be consistently lower under axial loading than was the case for corresponding figures for off-axis loading. Under off-axis loading conditions, the maximum tensile and compressive stresses, in general, were concentrated on the palatal and labial side of the implant neck within the cortical bone. In general, compressive stresses were more substantial than tensile stresses.

**Table 2** Principle Stresses (MPa) Arising in the Bone Around the Implant Under Axial and Off-Axis Loads

Bone type/ loading angle	Cortical bone		Cancellous bone	
	Max	Min	Max	Min
High density				
0 degrees	6.1	-13.6	2.8	-4.5
30 degrees	30.6	-54.0	3.8	-6.9
60 degrees	79.5	-95.6	6.2	-7.9
Low density				
0 degrees	10.8	-19.4	2.4	-3.9
30 degrees	31.6	-64.6	3.6	-5.9
60 degrees	87.7	-109.3	5.6	-6.6

## DISCUSSION

The significant and impressive success rates for dental implants suggest that tissues are capable of sustaining a long-term positive response to implant loading. This implies that bony architectural strength and the direction in which stresses are transferred to the surrounding bone are typically favorable as regards bone survival and impact stability.<sup>30,31</sup> At

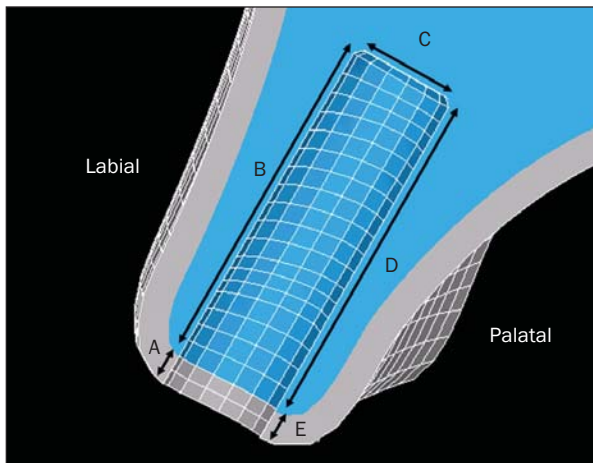
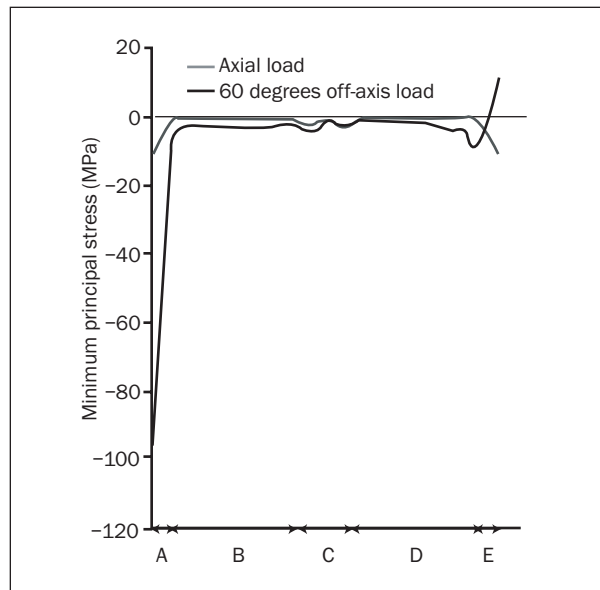
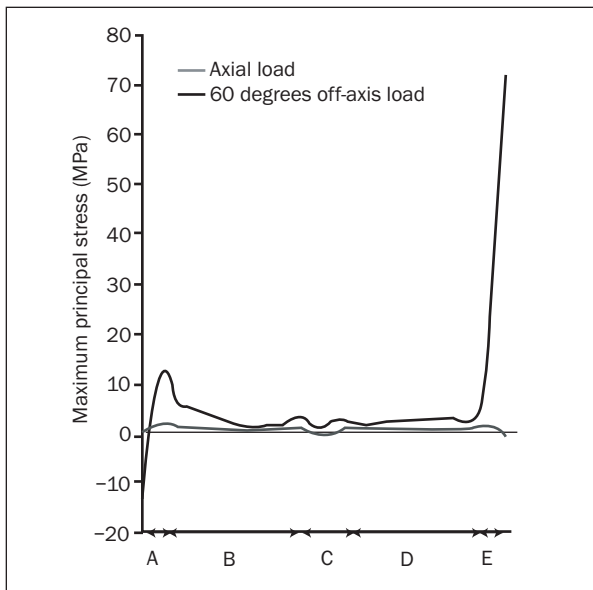


**Fig 7** Sagittal view of bone model. A = labial cortical bone region, B = labial cancellous bone region, C = implant apex area, D = palatal cancellous bone region, E = palatal cortical bone region.



**Figs 8a and 8b** Under axial and 60-degree off-axis loading, the (left) maximum and (right) minimum principal stresses arising at the implant-bone interface for high-density bone are displayed labially to palatally. A = labial cortical bone region, B = labial cancellous bone region, C = implant apex area, D = palatal cancellous bone region, E = palatal cortical bone region.

excessively high strains and/or numbers of chewing cycles, bone fatigue can occur, as has been reported previously.<sup>32,33</sup> Such a fatigue response can cause structural weakening of the bone if developing cracks are not repaired through ongoing bone remodeling.<sup>34</sup> In some cases, however, a clinician may need to introduce an implant-supported prosthesis in areas of compromised bone morphology, which may result in the development of an unfavorable off-axis load. An off-axis force could induce a bending moment and thus exert stress gradients within the implant as well as the adjacent bone. Given that the bone quality in the premaxillary region is not as high as that in the mandible, it was important to investigate how these off-axis forces could affect the stress distribution in bone of different quality.

Many different methods have been used to study the stresses/strains in bone and dental implants. For example, photoelasticity provides good qualitative information pertaining to the overall location of stresses but only limited quantitative information. Strain-gauge measurements provide accurate data regarding strains only at the specific location of the gauge.<sup>31,35</sup> FEA is capable of providing detailed quantitative data at any location within a mathematical model.<sup>29</sup> It would therefore appear that FEA could be a complementary tool for exploring the detailed mechanical responses at work in implant dentistry. Assumptions imposed on the FEA models (eg, regarding model geometry, load magnitude, load direction, and material property) influence the relative accuracy of the FEA. The use of a fine mesh is also

a major factor in the achievement of an accurate model in FEA.

In the present study, the occlusal force was assumed to be 178 N, the magnitude used in a previous 3D FEA of a maxillary anterior implant. This force was applied to an implant-supported prosthesis to simulate a real loading condition.<sup>29</sup> For dentate humans, in fact, the maximum bite force varies between individuals and different regions of the dental arch. With the bite force recorder used in the present study, average forces of more than 800 N for male young adults and 600 N for female young adults have been recorded in the molar region.<sup>36,37</sup> Smaller forces of 290 and 240 N, respectively, have been measured in the incisal region.<sup>36,37</sup> Different investigators have reported that the maximum incisal bite force ranges from 50 to 370 N.<sup>20,37,38</sup> The variation may be related to many factors, such as muscle size, bone shape, age, sex, degree of edentulism, and parafunction. However, the application of functional forces induces stresses and strains within the implant-prosthesis complex and affects the bone remodeling process around the implant.<sup>11,12</sup> Excessive forces on implant-supported prostheses could impair osseointegration or induce bone resorption.<sup>39-41</sup> Therefore, when evaluating the stresses and strains in the bone, it is essential to consider their source, the occlusal force. To reduce the risk of biomechanical overload and to increase the long-term success of the dental implant, the magnitude of the occlusal force, even the direction and the duration, must be considered in the treatment-planning stage.

In a comparative analysis, the complexity of real-life situations can be simplified, assuming that proportions and relative effects accurately reflect reality.<sup>42</sup> In the present study, the author varied the direction of the force to create an unfavorable loading situation in the anterior maxilla. In reality, unfavorable loading situations are more due to increased bone resorption after tooth loss. Varying the bone geometry and implant inclination according to various levels of maxillary resorption would have more accurately simulated situations observed clinically. Since the reconstruction of multiple complicated bone models was very elaborate and difficult, certain assumptions needed to be made to simulate unfavorable loading of an implant. Thus, the direction of the load was changed instead the bone geometry. However, a more valid assumption for the precise modeling of the geometry of the bone-implant system is needed for further study.

To get more reliable data, convergence tests with mesh refinements were performed. The mathematical model, which consists of more than 16,704 elements, revealed convergent results. The mesh used proved

sufficiently fine for the model. Sekine and coworkers measured the labiolingual mobility of 41 isolated osseointegrated implants in 8 human mandibles clinically using a displacement-measuring lever with electric strain gauges. The measuring point was 6 mm from the margin of bone shown on standardized x-rays of each implant. The load was increased linearly up to 20 N. They observed implant displacement of 17 to 58  $\mu\text{m}$  under a 20-N lateral load.<sup>43</sup>

So that the results of this FEA model could be compared with a real clinical situation, a similar load was applied to the test implant in the present study. The resulting level of implant displacement was 17  $\mu\text{m}$  for a high-density model and 19  $\mu\text{m}$  for a low-density bone model. The study revealed that the calculated load-displacement values were close to values reported for osseointegrated implants in vivo. The lower values were attributed to several assumptions that may have modified the outcome of the FEA model. The structures in the present models were all assumed to be homogeneous and isotropic. Additionally, 100% osseointegration at the implant-bone interface was simulated, which does not necessarily appropriately represent actual clinical situations. The stress distribution revealed was also consistent with the results of an FEA by Tada et al.<sup>22</sup> For low-density bone models utilizing a cylindrical implant, the maximum strain developed upon implant loading was observed around the implant apex.

Based on the results, the maximum equivalent stress/strain elicited by a force on this implant model appeared to increase linearly with an increase in the angle of loading from 0 to 60 degrees. For each 30-degree increase in loading angle, the maximum equivalent stress developed within the cortical bone increased an average of 3 to 4 times compared with that of an imparted axial load. Such a result would seem to indicate that load direction (upon an implant) exerts great influence upon the distribution of stresses within the supporting cortical bone.

EQV strain distribution in cancellous bone differed among the 6 different testing conditions, although in each case the maximum EQV strain was observed near the implant apex. Under the same loading angle, the EQV strain around the implant apex was higher in the low-density model than in the high-density model.

From the physiologic viewpoint, bone density is directly related to the strength and elastic modulus of bone<sup>44</sup>; thus, these results appear reasonable. The patterns of strain distribution within the bone were influenced not only by the load direction but also by bone quality. Furthermore, the maximum EQV strain was observed near the implant apex and not found at the cervical area of the implant. If a higher density

of the bone had been assumed in the study, the location of the maximum EQV strain distributed area would have been changed, as it did in a previous study.<sup>22</sup> Further research is needed to determine whether differences in bone quality resulting from differences in strain distribution may affect different mechanisms of failure.

Although the assumptions made for FEA models may still be too simplistic to be used to accurately predict the precise value of strains that arise within the bone around an implant, it appears of value to compare this study's calculated values with previously reported values. Based upon the mechanostat concept, peak load magnitudes creating strains greater than 4,000  $\mu$ strain would typically result in pathologic overload.<sup>14</sup> For the high-density bone model investigated herein, the maximum strain in the cortical bone was 3,410  $\mu$ strain; this strain was under 30-degree off-axis loading. It seemed that such strains would not be likely to result in pathologic overload. However, under 60-degree off-axis loading the maximum strain in the cortical bone model was 5,770  $\mu$ strain. Such strain would probably result in pathologic overload. Pathologic overload in bone may result in marginal bone loss and/or implant failure; hence, when off-axis loading is unavoidable, specific case-by-case selection of an implant location of appropriate bone quality is critically important.

The results of the present study showed that the force direction and bone quality were related to the stress/strain elicited along the implant-bone interface and the implant-abutment interface. Off-axis loading and poorer bone quality produced much more stress/strain than axial loading and better bone quality. Although many authors have postulated that osseointegrated dental implants have high success rates because of the development of excellent designs and procedures, elevated rates of complications and loss have been demonstrated after 5 years of function.<sup>45</sup> Despite little evidence that overloading can cause loss of osseointegration or bone resorption, some problems in clinical cases were solved by equilibration to achieve optimal occlusion and to avoid contact in lateral and protrusive movement.<sup>46</sup> Likewise many studies have demonstrated high survival rates for immediately loaded implants.<sup>6,47</sup> Glauser et al noted a 66% survival rate for implants placed in type 4 bone compared with a 91% survival rate for all other types of bone.<sup>48</sup>

Where possible, limiting the biomechanical effect of the provisional restoration by (a) limiting occlusal contact in central occlusion, (b) removing all excursive contacts, (c) limiting the effects of cantilever and off-axis loading, and (d) splinting implants together, has been suggested.<sup>49</sup>

## CONCLUSIONS

Based on 3-dimensional FEA of occlusal forces at various angles affecting the stress/strain distribution within different bone-quality types, the following conclusions can be drawn:

1. The maximum EQV stress/strain imparted to bone increased linearly with an increase in the angle of off-axis loading.
2. Under off-axis loading conditions, the maximum EQV stress generated was typically located buccally around the implant neck.
3. Different patterns of strain distribution occurred for different types of cancellous bone featuring different elastic moduli.

## REFERENCES

1. Eckert SE, Choi YG, Sanchez AR, Koka S. Comparison of dental implant systems: Quality of clinical evidence and prediction of 5-year survival. *Int J Oral Maxillofac Implants* 2005;20:406–415.
2. Perry J, Lenchewski E. Clinical performance and 5-year retrospective evaluation of Frialit-2 implants. *Int J Oral Maxillofac Implants* 2004;19:887–891.
3. Ferrigno N, Laureti M, Fanali S, Grippaudo G. A long-term follow-up study of non-submerged ITI implants in the treatment of totally edentulous jaws. Part I: Ten-year life table analysis of a prospective multicenter study with 1286 implants. *Clin Oral Implants Res* 2002;13:260–273.
4. Noack N, Willer J, Hoffmann J. Long-term results after placement of dental implants: Longitudinal study of 1,964 implants over 16 years. *Int J Oral Maxillofac Implants* 1999;14:784–755.
5. Luongo G, Di Raimondo R, Filippini P, Gualini F, Paoleschi C. Early loading of sandblasted, acid-etched implants in the posterior maxilla and mandible: A 1-year follow-up report from a multicenter 3-year prospective study. *Int J Oral Maxillofac Implants* 2005;20:84–91.
6. Ganeles J, Wismeijer D. Early and immediately restored and loaded dental implants for single-tooth and partial-arch applications. *Int J Oral Maxillofac Implants* 2004;19(suppl):92–102.
7. Esposito M, Hirsch JM, Lekholm U, Thomsen P. Biological factors contributing to failures of osseointegrated oral implants. (II). Etiopathogenesis. *Eur J Oral Sci* 1998;106:721–764.
8. Rosenberg ES, Torosian JP, Slots J. Microbial differences in 2 clinically distinct types of failures of osseointegrated implants. *Clin Oral Implants Res* 1991;2(3):135–144.
9. Tonetti MS. Determination of the success and failure of root-form osseointegrated dental implants. *Adv Dent Res* 1999;13:173–180.
10. Sahin S, Cehreli MC, Yalcin E. The influence of functional forces on the biomechanics of implant-supported prostheses—A review. *J Dent* 2002;30:271–282.
11. Bidez MW, Misch CE. Force transfer in implant dentistry: Basic concepts and principles. *J Oral Implantol* 1992;264–274.
12. Brånemark P-I, Zarb GA, Albrektsson T (eds). *Tissue-Integrated Prostheses: Osseointegration in Clinical Dentistry*. Chicago: Quintessence, 1985:129.
13. Cowin SC, Hegedus DA. Bone remodeling I: Theory of adaptive elasticity. *J Elast* 1976:313–326.

14. Frost HM. Bone "mass" and the "mechanostat": A proposal. *Anat Rec* 1987;219:1–9.
15. Frost HM. Bone's mechanostat: A 2003 update. *Anat Rec A Discov Mol Cell Evol Biol* 2003;275:1081–1101.
16. De Smet E, van Steenberghe D, Quirynen M, Naert I. The influence of plaque and/or excessive loading on marginal soft and hard tissue reactions around Brånemark implants: A review of literature and experience. *Int J Periodontics Restorative Dent* 2001;21:381–393.
17. Skalak R. Biomechanical considerations in osseointegrated prostheses. *J Prosthet Dent* 1983;49:843–848.
18. Tepper G, Haas R, Zechner W, Krach W, Watzek G. Three-dimensional finite element analysis of implant stability in the atrophic posterior maxilla: A mathematical study of the sinus floor augmentation. *Clin Oral Implants Res* 2002;13:657–665.
19. Holmes DC, Haganman CR, Aquilino SA. Deflection of superstructure and stress concentrations in the IMZ implant system. *Int J Prosthodont* 1994;7:239–246.
20. Osborn JW, Mao J. A thin bite-force transducer with three-dimensional capabilities reveals a consistent change in bite-force direction during human jaw-muscle endurance tests. *Arch Oral Biol* 1993;38:139–144.
21. Weinberg LA. Therapeutic biomechanics concepts and clinical procedures to reduce implant loading. Part I. *J Oral Implantol* 2001;27:293–301.
22. Tada S, Stegaroiu R, Kitamura E, Miyakawa O, Kusakari H. Influence of implant design and bone quality on stress/strain distribution in bone around implants: A 3-dimensional finite element analysis. *Int J Oral Maxillofac Implants* 2003;18:357–368.
23. Sevimay M, Turhan F, Kilicarslan MA, Eskitascioglu G. Three-dimensional finite element analysis of the effect of different bone quality on stress distribution in an implant-supported crown. *J Prosthet Dent* 2005;93:227–234.
24. Ishigaki S, Nakano T, Yamada S, Nakamura T, Takashima F. Biomechanical stress in bone surrounding an implant under simulated chewing. *Clin Oral Implants Res* 2003;14:97–102.
25. Fanuscu MI, Chang TL. Three-dimensional morphometric analysis of human cadaver bone: Microstructural data from maxilla and mandible. *Clin Oral Implants Res* 2004;15:213–218.
26. Chen J, Lu X, Paydar N, Akay HU, Roberts WE. Mechanical simulation of the human mandible with and without an endosseous implant. *Med Eng Phys* 1994;16:53–61.
27. Lozada JL, Abbate MF, Pizzarello FA, James RA. Comparative three-dimensional analysis of two finite-element endosseous implant designs. *J Oral Implantol* 1994;20:315–321.
28. Carter DR, Spengler DM. Mechanical properties and composition of cortical bone. *Clin Orthop Relat Res* 1978(135):192–217.
29. Clelland NL, Lee JK, Bimbenet OC, Brantley WA. A three-dimensional finite element stress analysis of angled abutments for an implant placed in the anterior maxilla. *J Prosthodont* 1995;4:95–100.
30. Morgan EF, Keaveny TM. Dependence of yield strain of human trabecular bone on anatomic site. *J Biomech* 2001;34:569–577.
31. Sahin S, Cehreli MC, Yalcin E. The influence of functional forces on the biomechanics of implant-supported prostheses—A review. *J Dent* 2002;30:271–282.
32. Gray RJ, Korbacher GK. Compressive fatigue behaviour of bovine compact bone. *J Biomech* 1974;7:287–292.
33. Swanson SA, Freeman MA, Day WH. The fatigue properties of human cortical bone. *Med Biol Eng* 1971;9:23–32.
34. Burr DB, Forwood MR, Fyhrie DP, Martin RB, Schaffler MB, Turner CH. Bone microdamage and skeletal fragility in osteoporotic and stress fractures. *J Bone Miner Res* 1997;12:6–15.
35. Brosh T, Pilo R, Sudai D. The influence of abutment angulation on strains and stresses along the implant/bone interface: Comparison between 2 experimental techniques. *J Prosthet Dent* 1998;79:328–334.
36. Waltimo A, Kemppainen P, Kononen M. Maximal contraction force and endurance of human jaw-closing muscles in isometric clenching. *Scand J Dent Res* 1993;101:416–421.
37. Waltimo A, Kononen M. Bite force on single as opposed to all maxillary front teeth. *Scand J Dent Res* 1994;102:372–375.
38. Paphangkorakit J, Osborn JW. The effect of pressure on a maximum incisal bite force in man. *Arch Oral Biol* 1997;42:11–17.
39. Isidor F. Loss of osseointegration caused by occlusal load of oral implants. A clinical and radiographic study in monkeys. *Clin Oral Implants Res* 1996;7:143–152.
40. Isidor F. Histological evaluation of peri-implant bone at implants subjected to occlusal overload or plaque accumulation. *Clin Oral Implants Res* 1997;8:1–9.
41. Quirynen M, Naert I, van Steenberghe D. Fixture design and overload influence marginal bone loss and fixture success in the Brånemark system. *Clin Oral Implants Res* 1992;3:104–111.
42. Meijer HJ, Starmans FJ, Bosman F, Steen WH. A comparison of three finite element models of an edentulous mandible provided with implants. *J Oral Rehabil* 1993;20:147–157.
43. Sekine H, Komiyama Y, Hotta H, Yoshida Y. Mobility characteristics and tactile sensitivity of osseointegrated fixture-supporting systems. In: van Steenberghe D (ed). *Tissue Integration in Oral Maxillofacial Reconstruction*. Amsterdam: Elsevier, 1986:306–332.
44. Misch CE, Qu Z, Bidez MW. Mechanical properties of trabecular bone in the human mandible: Implications for dental implant treatment planning and surgical placement. *J Oral Maxillofac Surg* 1999;57:700–706.
45. Lang NP, Berglundh T, Heitz-Mayfield LJ, Pjetursson BE, Salvi GE, Sanz M. Consensus statements and recommended clinical procedures regarding implant survival and complications. *Int J Oral Maxillofac Implants* 2004;19(suppl):150–154.
46. Vigolo P, Givani A, Majzoub Z, Cordioli G. Clinical evaluation of small-diameter implants in single-tooth and multiple-implant restorations: A 7-year retrospective study. *Int J Oral Maxillofac Implants* 2004;19:703–709.
47. Chiapasco M. Early and immediate restoration and loading of implants in completely edentulous patients. *Int J Oral Maxillofac Implants* 2004;19(suppl):76–91.
48. Glauser R, Ree A, Lundgren A, Gottlow J, Hammerle CHF, Schärer P. Immediate occlusal loading of Brånemark implants applied in various jawbone regions: A prospective, 1-year clinical study. *Clin Implant Dent Relat Res* 2001;3:204–213.
49. Morton D, Jaffin R, Weber HP. Immediate restoration and loading of dental implants: Clinical considerations and protocols. *Int J Oral Maxillofac Implants* 2004;19(suppl):103–108.

---

## Erratum

In the article, "A Novel Drilling Procedure and Subsequent Bone Autograft Preparation: A Technical Note," by Anitua et al (*Int J Oral Maxillofac Implants* 2007;22:138–145), Fig 1h should have illustrated the placement of the implant rather than the use of the countersink drill. This error has been corrected in the online version of the article, which is available at [www.quintpub.com](http://www.quintpub.com). The JOMI staff regrets the error.